Egyptian Journal of Chemistry

http://ejchem.journals.ekb.eg/

Kinetics of immobilized alpha amylase impregnated with silver nanoparticles in Egg membrane for enhanced starch hydrolysis

Halima R[a*] and Archna Narula[b]

[a]*Department of Biotechnology, Sir M Visvesvaraya Institute of Technology, Bangalore-562157,India*

[b]*Department of Chemical Engineering, M.S Ramaiah Institute of Technology, Bangalore-560054,India*

Abstract

In this study, α-amylase, an industrially important enzyme was successfully immobilized on a porous egg membrane impregnated with silver nanoparticles and has been used for starch hydrolysis reaction. The immobilized alpha-amylase impregnated with silver nanoparticles on an egg membrane (IAmy/IAg-Np/ESM) was studied for its catalytic efficacy using starch as a substrate under variable reaction conditions viz. pH, temperature, and substrate concentration. The results were compared with that of reaction with free nanoparticles and free amylase enzyme. IAmy/IAg-Np/ESM showed highest *Km* and *Vmax* values (2.2 and 1.7-fold) and lower *Vmax/Km* ratio (1.4-fold), respectively in comparison to the free enzyme. The enzyme with free nanoparticles showed higher *Km* and *Vmax* values (1.7 and 1.1-fold) and lower *Vmax/Km* ratio (1.2-fold), respectively in comparison to free enzyme. IAmy/IAg-Np/ESM and the enzyme with free nanoparticles the free enzyme, exhibited lower activation energy, higher D-values, higher half-life, lower deactivation constant rate, and higher energy for denaturation in comparison with free enzyme. Immobilization of α-amylase increased enthalpy & free energy and decreased entropy of thermal inactivation. Similar behavior was exhibited by the enzyme with free nanoparticles. A significant increase in pH stability of IAmy/IAg-Np/ESM was observed especially at alkaline pH values. IAmy/IAg-Np/ESM membrane was characterized by SEM and FTIR for structural properties.In addition, IAmy/IAg-Np/ESM preserved 100% of its initial activity after 15 consecutive usages in the reaction. The residual activity of enzyme was 80% at 4 °C after 21 days of storage. The enzyme with free nanoparticles improved the kinetic properties. The immobilization process improved the catalytic properties and stabilities, thus increasing the suitability for industrial processes with lower cost and time.

Keywords : Green synthesis, immobilized silver nanoparticles, Egg membrane, Enzyme kinetics, stability of membrane

1. Introduction

Enzymes are slowly but steadily gaining relevance as biocatalysts in a variety of industries, from food to pharmaceuticals. The enzymatic method has a number of advantages, including low toxicity, selectivity, and the acceleration of mild reaction conditions with high yield and exclusivity towards the target products [1]. α-amylase catalyses the breakdown of the starch molecule's α-D-1,4 glucosidic bonds, resulting in dextrin and other glucose-based polymers. Textile, culinary, baking, detergent, brewing, pharmaceutical, and clinical chemistry are just a few of the areas where α-amylases are used [2,3]. Despite their importance, amylases face challenges such as high sensitivity to harsh industrial process conditions, limited stability, short lifetime, and difficulties in recovery, all of these raise manufacturing costs. Enzyme immobilization is one of the most effective strategies for resolving these issues since it not only stabilizes enzymes under operational circumstances but also allows for easy recovery and reusability for multiple times [4]. Covalent binding, physical adsorption, entrapment, and cross linking to solid carriers are all techniques for immobilizing enzymes. Covalent binding is regarded to be the most successful method. The establishment of covalent connections between the enzyme and the carrier surface may be a helpful approach for generating enzymes and preventing their leaching and subsequent leakage [5]. Physical adsorption is the most common, easiest to do, and oldest method. Because of the weak connections between the enzyme and the carrier surface (as van der Waals, hydrogen bonding, hydrophilic/ hydrophobic, and electrostatic interactions), the immobilised enzyme through physical adsorption has low stability after repeated use. To improve the stability of immobilised enzymes, a technique

*Corresponding author e-mail: halimajenish@gmail.com

Receive Date: 12 December 2021, Revise Date: 10 April 2022, Accept Date: 27 May 2022

DOI: 10.21608/EJCHEM.2022.110860.5050

combining the advantages of physical adsorption and covalent binding was proposed [6]. Immobilization can involve a variety of organic and inorganic carriers, each with its own set of properties that influence the enzyme's behaviour. The enormous surface area of the nano-carrier aids in the reduction of diffusion barriers in the transfer of the substrate and reaction products, boosting the effectiveness of the immobilised enzyme [7].

The resistance of a folded protein shape to thermal denaturation is referred to as thermodynamic stability. The thermodynamic characteristics of enzymes are used to determine their appropriateness for industrial use. Variations in thermodynamic parameters like as enthalpy, entropy, and the Gibbs free energy can reveal a lot about an enzyme's activity, behaviour, and thermo-stability. Furthermore, studying the kinetic and thermodynamic features of bio-nanocatalysts is critical for developing a highly effective immobilized enzyme [8].

In the current study the α-amylase is immobilized on egg membrane impregnated with silver nanoparticles to increase the stability and activity. This membrane was used in the reaction with starch as a substrate to study its activity. The experiments were conducted at variable pH, temperature and substrate concentrations to study the stability of its activity. Comparative study including catalytic, kinetic and thermodynamic parameters for free enzyme, free enzyme with free nanoparticles and immobilized enzymes impregnated with silver nanoparticles was carried out. The stability along with the reusability of the membrane over various pH and temperature ranges was studied to explore the possible usage of the membrane for industrial application.

2. Experimental

Materials

Soluble starch was used as a substrate for the amylase reaction. The soluble starch (AR grade) was procured from Sigma Aldrich. The enzyme α-amylase used in the reaction was purified enzyme extracted from malt and procured from Himedia. 3, 5-dinitrosalicylic acid (DNS) (AR grade) is procured from Sigma Aldrich and used in enzymatic assays. The broiler egg shells were collected from the waste generated by local vendors' waste. The egg shells were washed thoroughly 3-4 times with running tap water to remove unwanted contaminants and dried in hot air oven. The egg shells are then dipped in dilute HCl solution (20%) to isolate the membrane from the shells

Enzyme Assay

To measure α-amylase activity 0.5 ml of 1% soluble starch (w/w) was added to 0.1 M phosphate buffer (pH 7.0) and combined with 0.5 ml of enzyme. The reaction mixture was incubated at 40° C for 30 minutes [9]. The reaction was arrested by adding 1 mL of dinitrosalicysilic acid (DNS) reagent and heating for 10 minutes over a boiling water bath [10]. At 540 nm the absorbance was measured. All experiments were conducted in triplicate and results were expressed as average values.

Determination of Protein content

The method of [11] was used to estimate protein using bovine serum albumin (BSA) procured from HIMEDIA as a standard.

Green synthesis of Silver Nanoparticle

The green synthesis of AgNp was carried out under optimized condition from *Piper betle* leaf extract. To prepare the leaf extract 10 gms of fresh leaves were crushed in a mortar and pestle using distilled water. The extract was filtered through Whatman No.1 filter paper and diluted to 100mL. 10 ml of 0.1 mM $AgNO_3$ solution was added to 90 mL of prepared leaf extract. The mixture was exposed to sunlight for 20 mins for the complete reduction of $AgNO_3$ solution to silver nanoparticles. The reduction activity indicated the formation of AgNps. The AgNps produced were collected by centrifuging at 10,000rpm for 10 mins (REMI). The further confirmation of silver nanoparticles was done using SEM**.**

Extraction of Egg membrane

The egg membrane was removed from egg shell by dipping the egg shell in diluted HCl solution for about 10 mins. During this duration of 10 mins, the calcium carbonate in the egg shell reacted with HCl to form calcium chloride and carbon dioxide; as a result the membrane was separated from egg shell. Subsequently the membrane was washed with distilled water to remove any traces of acid and to neutralize the membrane.

Impregnation of silver nanoparticles on egg membrane

The membrane was then dipped in 10 mM $AgNO_3$ solution for 10 mins, followed by washing with distilled water to remove the excess traces of $AgNO_3$ solution. Egg membrane was then dipped in plant extract for about 10 mins. The colour of the egg membrane changed from white to brown indicating the presence of silver nanoparticles on the membrane.

Immobilized Alpha Amylase Impregnated with Silver Nanoparticles on Egg Membrane (Iamy/Iag-Np/ESM)

The silver nanoparticles impregnated egg membrane was immersed in 1% alpha amylase solution overnight for about 8 hrs at 4°C. The α-amylase got

immobilized on the egg membrane with was already impregnated with silver nanoparticles. Figure 1 demonstrates the step wise mechanism of synthesizing immobilized alpha amylase on egg membrane impregnated with silver nanoparticles (Iamy/Iag-Np/ESM).

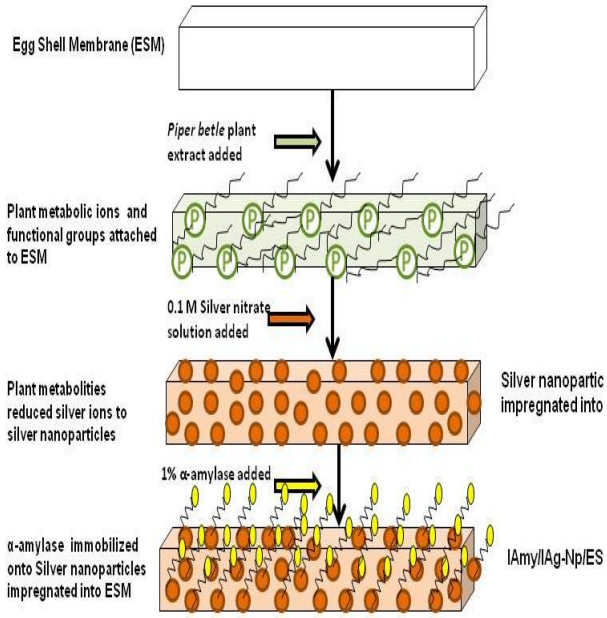

Figure 1: Mechanism of preparation of immobilized alpha amylase on egg membrane impregnated with silver nanoparticles (Iamy/Iag-Np/ESM)

Characterisation of Iamy/Iag-Np/ESM:

FTIR (Fourier transforms infrared spectroscopy) analysis:

The FTIR absorption spectra of plant extract, α-amylase, free silver nanoparticles and Iamy/Iag-Np/ESM were measured by FTIR spectroscopy using Bruker model Alpha ATR with wave number range from 400- 4000cm^{-1}. The analysis was used to determine the functional group and carbonyl group formed. The sample was scanned over a wave number range of 400–4000 cm^{-1} and the characteristic peaks were recorded.

SEM

Morphological examination of the surfaces of egg membrane, synthesized silver nanoparticles and Iamy/Iag-Np/ESM were carried out using on a Carl Zeiss ultra 55 SEM with Oxford EDS detector. A small sample was loaded on a carbon coated copper grid to create, a thin film for study.

Nanocatalytic enzymatic assay

The dinitrosalicylic (DNS) acid method was used to perform the α-amylase enzymatic assay. The assay was performed with purified α-amylase enzyme. Three different reaction assays were investigated, *viz.* free enzyme, enzyme with free silver nanoparticles, and Iamy/Iag-Np/ESM. For all the three reactions starch was used as a substrate. The three reactions were carried out in boiling tubes with 10 ml of the reaction mixture, 1 ml of enzyme (purified enzyme, enzyme with free nanoparticles, Iamy/Iag-Np/ESM (1x1 cm dimension membrane)) and 1 ml of starch with 8 ml of phosphate buffer (pH 7.0). The above reactions were carried out in triplicates at 28 ± 2 °C for 10 minutes. The reaction was then arrested by DNS solution and heating the reaction tubes in a boiling water bath. The levels of free glucose were calculated for α-amylase activity and expressed in International Units (IU), using a colorimeter. The amount of α-amylase enzyme with silver nanoparticles required to release 1 µ mol of glucose under experimental conditions was referred to as released glucose.

Effect of time on amylase activity:

The time of reaction of the enzyme α-amylase to hydrolyse the substrate starch was determined using DNS assay. The rate of reaction was determined at variable time intervals viz. 2, 4, 6, 8, 10, 12, 14 and 16 mins and the *Km* value was calculated using the equation 1. The experiment was repeated for enzyme with free silver nanoparticles and Iamy/Iag-Np/ESM

$K=2.303\log[A_\infty-A_0/A_\infty-A_T]/t$…….(1)

Where, A_∞ the amount of maltose liberated at n^{th} minute, A_0 the amount of maltose liberated at zeroth minute, A_T the amount of maltose liberated at time t and t is the time of reaction.

Effect of temperature on amylase activity:

The optimum temperature of α-amylase activity was measured by conducting the reaction at different temperatures viz. 20˚C, 30˚C, 40˚C, 50˚C, 60˚C and 70˚C and enzyme assays were performed. The activation energy (E_a) of both free and immobilized α-amylase were calculated from the slope of the Arrhenius plot according to the following equation:

Slope = (- E_a / 2.303) x R…… (2)

Where: *R* is gas constant (8.314 KJ/mol).

Effect of pH on amylase activity:

The effect of pH on enzyme activity (pure enzyme, enzyme with silver nanoparticles and Iamy/Iag-Np/ESM) was examined by performing the enzyme assay at different pH values of 3,4,5,6,7,8,9,10 and 11 by using 0.1 M of the following buffer systems: citrate-phosphate buffer (pH 5.0–6.0), sodium phosphate (pH 7.0-8.0) and glycine NaOH (pH 9.0-11.0) [18]. Enzyme activity was measured at varied pH range and the optimum assay conditions for pH were determined.

Effect of substrate concentration on amylase activity:

For estimation of optimum substrate concentration

for maximum α-amylase enzymatic activity (pure enzyme, enzyme with silver nanoparticles and Iamy/Iag-Np/ESM) was assayed with different volumes of 1% soluble starch concentrations (0.2, 0.4, 0.6, 0.8, 1.0, 1.2, 1.4, 1.6, 1.8 and 2 %). The enzyme kinetic parameters, Michaelis–Menten constant (*Km*), and maximum reaction velocity (*Vmax*) were determined at optimum assay conditions [19]. The rate of reaction when the enzyme is saturated is, Vmax. Km, is the substrate concentration when the initial velocity, V_0= *Vmax*/2. The catalytic efficiency (*Vmax/Km)* of α-amylase was determined to demonstrate the affinity of enzyme to substrate.

Thermal stability:

Thermal stability of the free enzyme, enzymes with free nanoparticles and Iamy/Iag-Np/ESM was determined by incubating the enzyme at various temperature ranges from 60°C to 90°C for 60 min in the absence of substrate. Samples were taken at 15 min intervals and assayed for activity under optimized conditions. The residual activity was calculated by taking the enzyme activity at 0 min incubation as 100 %:

Residual activity (RA%) = (Final activity/ Initial activity) x100……. (3)

The thermal and thermodynamic constants were calculated as [20]. Deactivation rate constant (K_d) equals to slope of Arrhenius plot of log RA (%) against time (min)

Slope = - K_d…….(4)

The enzyme half-life time ($t_{1/2}$) corresponds to the time period necessary for the residual activity to decrease by 50 % of its initial value.

$t_{1/2}$ = ln 2/ K_d ……(5)

Decimal reduction time (D-value) is the time required to lower the initial activity by 90% at a certain temperature.

D-value = ln10/ K_d……..…….(6)

Slope of plot of denaturation rate constants (ln Kd) vs reciprocal of absolute temperature (K) was used to calculate the activation energy (Ed)

Slope = -E_d / R ……(7)

The change in enthalpy (ΔH°, kJ/mol), free energy (ΔG° kJ/mol) and entropy (ΔS°, J/mol/ K) for thermal denaturation of α-amylase were determined using the following equations:

$\Delta H^\circ = E_d - RT$…….(8)

ΔG°= -RT ln (K_d x h / K_b x T)…….. (9)

$\Delta S^\circ = (\Delta H^\circ - \Delta G^\circ) / T$…… (10)

Where: E_d is the activation energy for denaturation (KJ/mol)), R is the gas constant(8.314 J/mol/K), T is the absolute temperature (K), K_d is the deactivation rate constant (/min), h is the Planck constant (11.04 x 10^{-36} J min) and K_b is the Boltzman constant (1.38 x 10^{-23} JK).

pH stability:

After pre-incubating the enzyme for 60 minutes at 30° C with 0.1 M buffer systems at different pH ranges (pH 5.0-11.0) without substrate, the pH stability of the free and immobilised α-amylase was measured. The enzyme activity was evaluated every 30 minutes, and the pH stability was calculated as a percentage of the original enzyme activity at 0 minutes incubation.

Operational stability (reusability):

The reusability of immobilized α-amylase (Iamy/Iag-Np/ESM) was studied for several cycles and the RA % was determined. After each cycle, the membrane was washed to remove any residual substrate with sodium phosphate buffer (0.1 M, pH 8.0) and was reused for the new cycle. The activity in the first run was taken as 100 % and the RA was expressed as a percentage of the starting operational activity.

Storage stability:

The membrane was stored at 4°C for 21 days and the residual activity was measured under optimal conditions.

3. Results and Discussion

Green synthesis of silver nanoparticles:

The mixture of $AgNO_3$ and leaf extract solution turned from pale yellow colour to brown colour indicating the reduction in activity and thereby the presence of AgNps. The plant metabolites present in the extract play a vital role in the reduction of the metal ions [35].The shape of the AgNp synthesized was found to be spherical and of size 41nm was observed (figure 2 a))

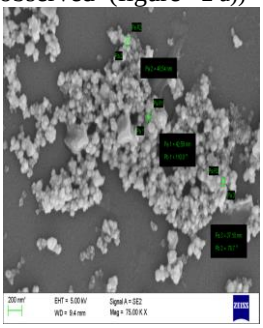

2a)

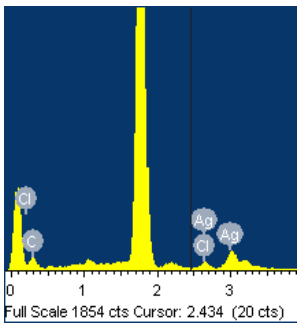

2b)

Figure 2: a) SEM image of the silver nanoparticle b) EDX profile of the silver nanoparticle.

Figure 2 b) shows the EDX profile of the synthesized silver nanoparticles. The characteristic peak of Ag in EDX confirms the presence of silver nanoparticles. The elemental composition by EDX shows the presence of silver and chlorine suggesting the presence of nanoscale silver chloride (AgCl)

particles. The percentage of silver (Ag) is 23.45% and Chlorine (Cl) ions is 9.05% in the membrane is found through EDX. The chloride ions present in the membrane are because of the treatment before subjecting to SEM analysis.

Immobilization of AgNps on an egg membrane:
The egg membrane slowly turned from white to brown colour on incubation with the plant extract, indicating the formation of silver nanoparticles on the membrane surface. Figure 3 shows the colour change of the membrane on timely basis (from 0 to 10 mins).

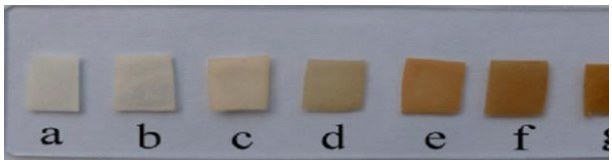

Figure 3: Immobilization of AgNps in Egg membrane

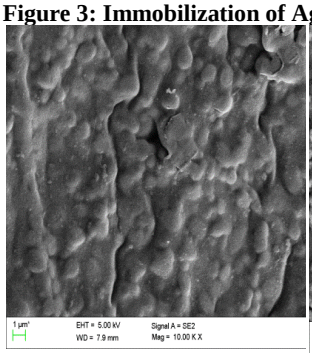

4a)

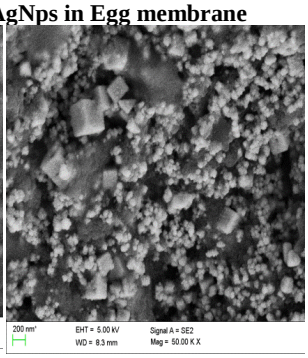

4b)

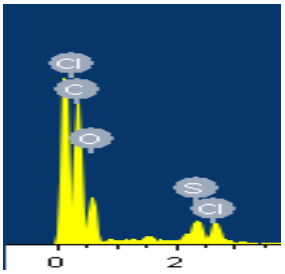

4c)

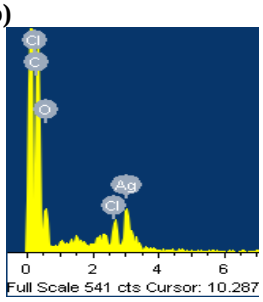

4d)

Figure 4: SEM image of a) Egg membrane b) Egg membrane with immobilized alpha amylase and impregnated AgNp from Piper betle c) EDX profile of egg membrane d) EDX

Figure 4 a) shows the egg membrane before immobilizing where there is no nanoparticle formation. The corresponding EDX shows the absence of Ag. Figure b) shows the immobilized egg membrane with AgNp. The shape of the particles was found to be cube with a size of 77nm. The corresponding EDX shows the presence of Ag in the membrane. The presence of Cl in EDX is due to the sample pretreatment before subjecting to SEM. In figure 1 a) the size of the silver nanoparticle formed form the *Piper betle* plant extract is found to be 42 nm whereas after the membrane is processed with the plant extract and amylase nanoparticles, size is observed to be 77nm. The substantial increase in nanoparticles size from 41nm to 77 nm, confirms that alpha amylase was immobilized with the silver nanoparticle that were impregnated on the egg membrane.

FTIR
FT-IR spectroscopic analysis of (a),Plant Extract (b), silver nanoparticles (c), egg membrane and (d) Iamy/Iag-Np/ESM were carried out for the wave number 400 – 4000 cm^{-1} (Fig. 5). Figure 5 a) shows the characteristic absorption bands of *Piper betle* at
3345 cm^{-1} (corresponding to NH_2 group), 1653 cm^{-1} (N-H bending vibrations) and at 534 cm^{-1} (O-H bending and vibrations), which was in accordance with literature. Figure 5 b) shows the widening of the peaks, and a shift of peak was observed from 1626 cm^{-1} to 1653 cm^{-1} corresponding to the C = N-.The broadening of the peak observed at 515 cm^{-1} , shows the plant metabolite has influenced the production of the nanoparticles. Figure 5 c) shows the FTIR image of egg membrane which has peak of 3258 cm^{-1} (O-H and N-H stretching vibrations), 2915 cm^{-1} (C-H stretching vibrations) ,1626 cm^{-1} corresponds to (C = N-) group , 1510 cm^{-1} HCH interactions (not occurring in the rings) , 1388 cm^{-1} (C-N stretching vibrations) 1224 cm^{-1} (CC stretching).The egg membrane with immobilized α-amylase with impregnated silver nanoparticles shows the typical peak broadening at 3270 cm^{-1} and peak modification at 1626 cm^{-1} corresponding to the (C = N-) to 1632 cm^{-1} which shows additional groups were added , 1510 cm^{-1} (resulting from HCH interactions) to 1544 cm^{-1} where CCH and CC modes are prevalent. This confirms that the silver nanoparticles and the α-amylase were incorporated to the membrane. The above data confirms that the process of processes of amination, activation, and immobilization were successful. The results were in agreement with the results obtained by other researchers [15].

Effect of time:
All proteins suffer saturation, and hence loss of catalytic activity with time. Enzyme catalyzed reactions are reversible [21]. Initially, there was little or no product present, and therefore the reaction proceeds only in the forward directions. However, as the reaction continues, there was a significant accumulation of product, and there was a significant rate of backward reaction. The rate of product formation slows down as the incubation proceeds, and if the incubation time was long then the measured activity of the enzyme would reduce. The longer an enzyme was incubated with its substrate, the greater was the amount of product that would be formed[22]. For the pure enzyme α-amylase activity (free enzyme) the reaction continued till 10 mins and then saturation was found indicating there was no product formation as all the active sites were bonded with substrate. Thus beyond 10 mins there was no possibility of hydrolysis reaction. The reaction with pure α-amylase and free nanoparticles showed saturation at 12 mins further to this there is no product formation and increased product formation. freeenzyme.

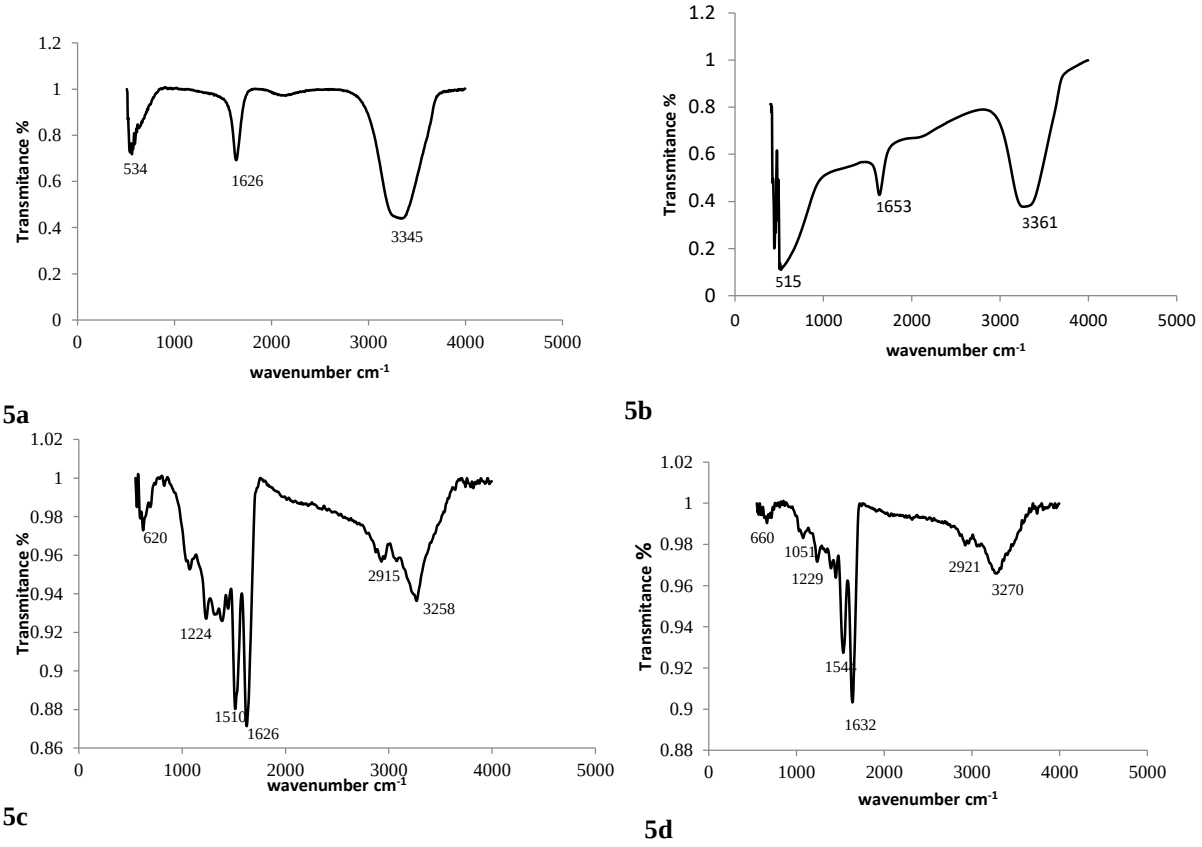

Figure 5: FTIR images of a) Plant extract b) Silver nanoparticles c) Egg membrane and d) IAmy/IAg-Np/ESM

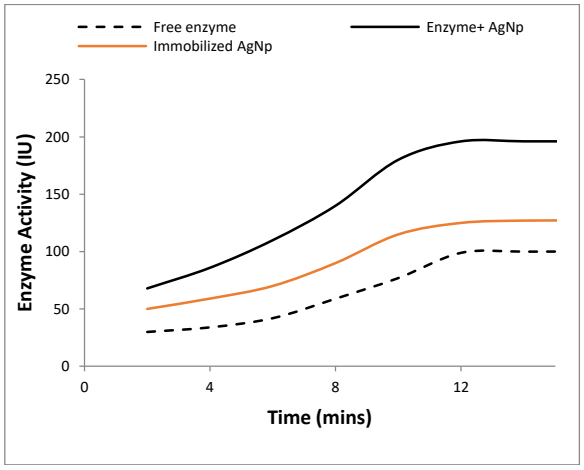

Figure 6: Effect of different time intervals on Enzyme activity with free enzyme, enzyme with nanoparticles and Iamy/Iag-Np/ESM

The silver nanoparticles present acted as a catalyst and had accelerated the reaction rate by exposing more active sites for the enzyme for binding. Whereas the reaction of immobilized amylase with impregnated silver nanoparticles showed the saturation at even 12 mins but an increased product was observed when compared with that of the other reaction methods as the membrane has accelerated the rate of reaction by exposing more active sites.

Effect of pH:

Changes in pH lead to the breaking of ionic bonds that holds the tertiary structure of the enzyme in place[23].Increasing hydrogen ion concentration increases the successful competition of hydrogen ions for any metal cationic binding sites on the enzyme, reducing the bound metal cation concentration. Decreasing hydrogen ion concentration increases hydroxyl ion concentration which competes against the enzyme ligands for divalent and trivalent cations causing their conversion to hydroxides. Thus enzyme begins to lose its functional shape, particularly the shape of the active site, such that the substrate no longer fits into it and the enzyme gets denatured [24].

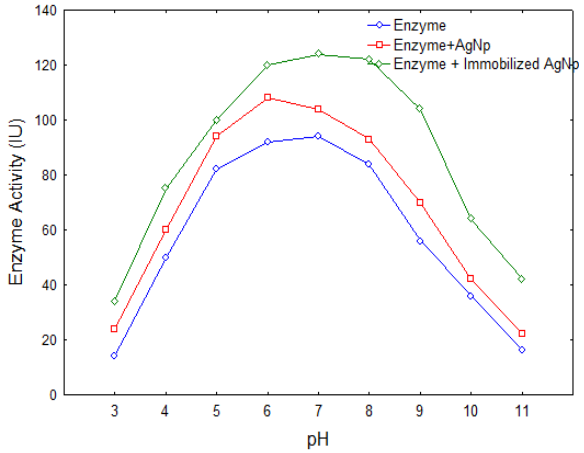

Figure 7: Effect of various pH on Enzyme Activity with free enzyme, enzyme with nanoparticles and Iamy/Iag-Np/ESM

From Figure 7 it is inferred that the optimum pH for the enzyme activity for free enzyme, enzyme with nanoparticles and Iamy/Iag-Np/ESM is 7. The reaction of Iamy/Iag-Np/ESM has the same activity and product formation at pH 8. This might be due to the acceleration of reaction rate in the presence of silver nanoparticles and the change of conformational structure of protein at higher pH due to immobilization.

Effect of temperature:

The temperature ranges over which the enzyme shows activity was limited between the melting point (0˚C) and boiling point (100˚C) of water. The rate of reaction increases initially with every 10˚C raise in temperature due to increase in kinetic energy. At elevated temperature the intra-molecular interactions between polar groups and the hydrophobic forces between the non polar groups results in thermal deactivation [25].

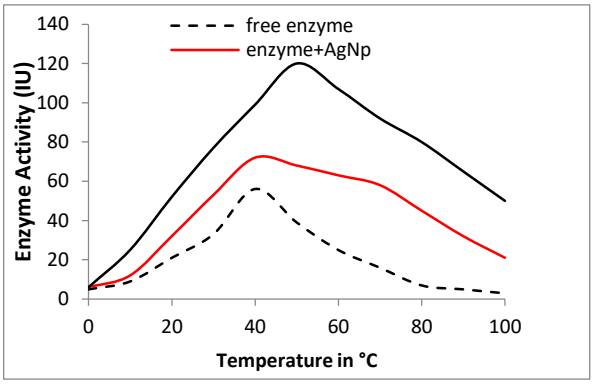

Figure 8: Effect of different Temperature on Enzyme activity with free enzyme, enzyme with nanoparticles and Iamy/Iag-Np/ESM

From Figure 9 it is understood that the activation energy is more with addition of silver nanoparticles and the immobilized amylase on impregnated membrane. The Ea of free enzyme is 5.14 KJ/mol for enzyme with free nanoparticles is 4.5 KJ/mol, and for immobilized enzyme in impregnated with silvernaoparticle membrane is 3.67 KJ/mol (Figure 9). This finding implied that immobilization improved enzyme catalytic efficiency by lowering the Ea required for the formation of an activated enzyme-substrate complex. Figure 8 shows that product formation is not affected at higher temperature for immobilized amylase with silver nanoparticles when compared to free enzyme. The immobilization of amylase has enabled better protection of heat sensitive free amylase at higher temperatures. The presence of silver nanoparticles enhances the enzyme activity thereby increasing the rate of reaction.

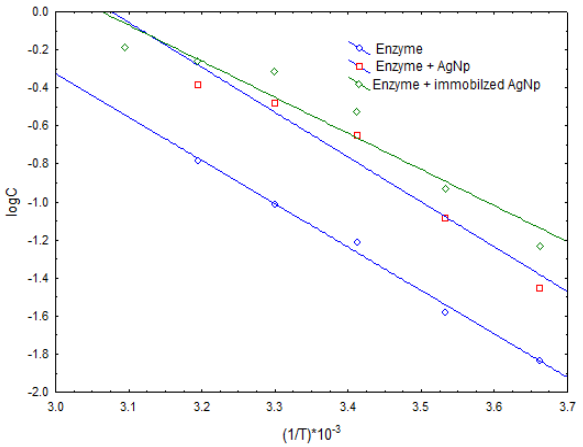

Figure 9: Log C graph of Enzyme activity with free enzyme, enzyme with nanoparticles and Iamy/Iag-Np/ESM

Effect of substrate concentration:

The catalytic site of the enzyme allows the substrate to bind and the rate of reaction is altered by the concentration of substrate added [27]. An enzyme with high K_m has a low affinity for its substrate and requires a greater concentration of substrate to achieve V_{max}.

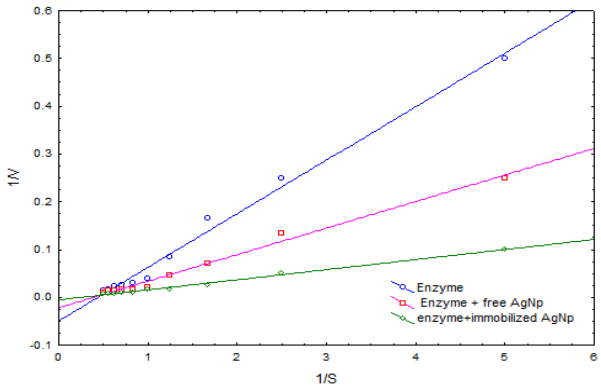

a)

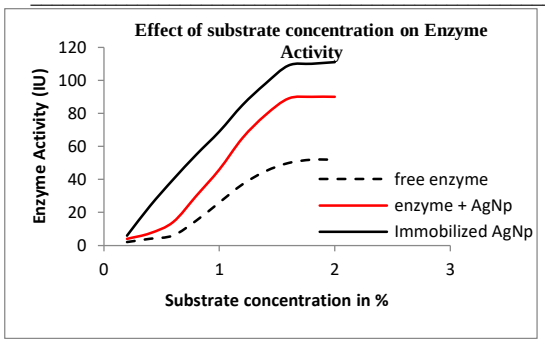

b)

Figure 10: a) Line-Weaver Burk (LB) plot and b) Effect of substrate on Enzyme Activity with free enzyme, enzyme with nanoparticles and Iamy/Iag-Np/ESM

Iamy/Iag-Np/ESM with varying substrate concentation

The enzyme activity increased with increasing starch concentration for enzyme with nanoparticles and Iamy/Iag-Np/ESM (Figure 10 b). The reaction kinetics of the free and Iamy/Iag-Np/ESM as estimated using Line-Weaver Burk (LB) plot under optimal conditions (Figure 10 a), indicate that the calculated *Km* value of the Iamy/Iag-Np/ESM was 2.2-fold higher than the free enzyme. The enzyme with free nanoparticles showed 1.7 fold higher values than that of the free enzyme. As *Km* increases the affinity of the substrate to the enzyme decreases, thereby lot of substrate is required to saturate the

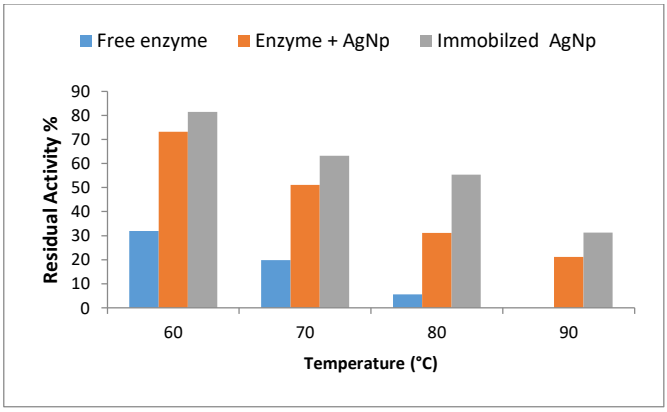

a)

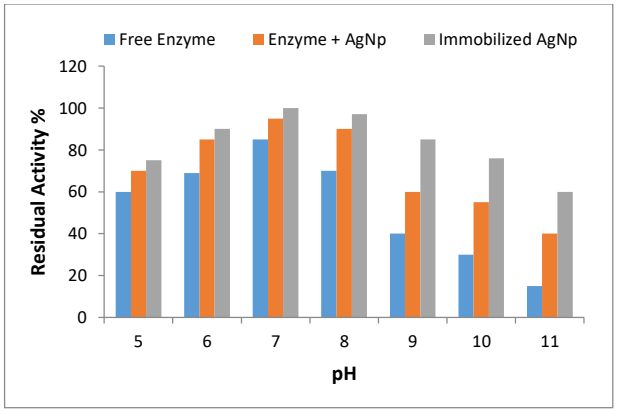

b)

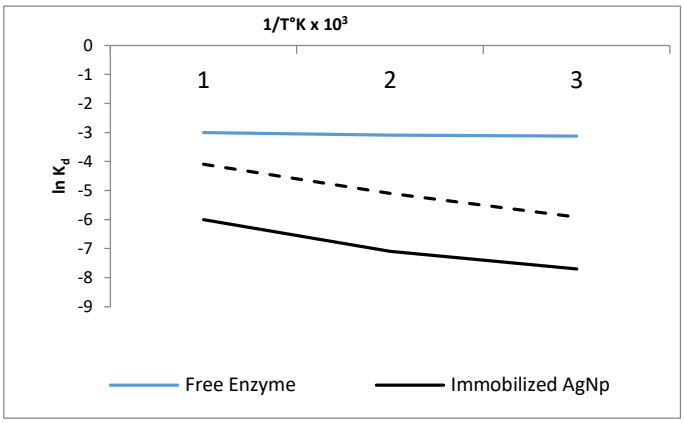

c)

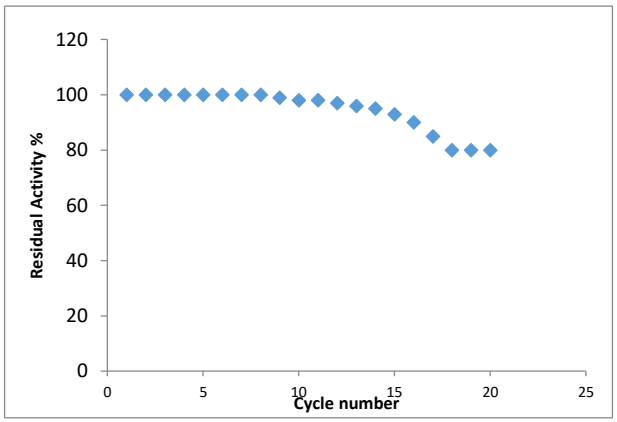

d)

Figure 11: Thermal stability (a), Arrhenius plot for energy of denaturation (Ed) (b), pH stability (c) and operational stability (d) of α-amylase enzyme.

Figure 10 a) shows the Line-Weaver Burk (LB) on Enzyme Activity with free enzyme, enzyme with nanoparticles and Iamy/Iag-Np/ESM . LB lot is the most commonly used plot for enzyme kinetics and b) show the substrate utilization of purified enzyme, purified enzyme with free nanoparticles, and enzyme. In addition, the *Vmax* of the Iamy/Iag-Np/ESM was higher than the value of the free form by 1.7-fold. Alternatively *Vmax* of the enzyme with free nanoparticles is found to be 1.1 fold higher for free enzyme. These effects could be due to changes in enzyme configuration caused by immobilisation. This indicated that the conversion rate of substrate to

product increased, but the affinity for substrate decreased, owing to a change in the microenvironment of the enzyme active site caused by immobilization. The Vmax/Km ratio for Iamy/Iag-Np/ESM was 1.3 fold lower than the free enzyme. The results indicated that immobilized enzyme has less specificity to the substrate. Singh et al reported that a reduction in enzyme kinetic parameters after immobilization can be related to conformational changes in its structure [22].

Table 1: Thermal inactivation kinetics and thermodynamic parameters of free enzyme, enzyme with free nanoparticles and Iamy/Iag-Np/ESM

Enzyme	E_d (KJ/mol)	Thermal inactivation parameters	Temperature (° C) 60	70	Thermodynamic parameters	Temperature(° C) 60	70
Free enzyme	23.42	K_d (min^{-1})	$10.25x\ 10^{-3}$	$11.55\ x\ 10^{-3}$	ΔH° (kJ/mol)	20.51	20.3
		$t_{1/2}$ (min)	63.60	58.99	ΔG° (kJ/mol)	92.66	94.09
		D-Value (min)	223.56	197.30	ΔS° (J/mol/^{0}K)	-0.21	-0.21
Enzyme with Free nanoparticles	65.79	K_d (min^{-1})	$0.12\ x\ 10^{-3}$	$0.21\ x\ 10^{-3}$	ΔH° (kJ/mol)	60.23	60.18
		$t_{1/2}$ (min)	998.42	678.41	ΔG° (kJ/mol)	96.54	98.78
		D-Value (min)	2178	1072	ΔS° (J/mol/^{0}K)	-0.10	-0.10
Iamy/Iag-Np/ESM	87.98	K_d (min^{-1})	$0.48\ x\ 10^{-3}$	$0.89\ x\ 10^{-3}$	ΔH° (kJ/mol)	84.21	84.13
		$t_{1/2}$ (min)	1462.98	775.34	ΔG° (kJ/mol)	101.21	103.31
		D-Value (min)	4793.15	2542.05	ΔS° (J/mol/^{0}K)	-0.06	-0.06

Thermal stability

Figure 11 a) explains the importance of immobilization process in enhancing the thermal stability of enzyme. The residual activity at 60°C after 60 min for the free enzyme, enzyme with free nanoparticles and Iamy/Iag-Np/ESM was 32 %, 73.12% and 91.37 % respectively. At higher temperatures and longer time duration, the residual activity of the free enzyme declined dramatically. Application of immobilization increased the thermal stability of Iamy/Iag-Np/ESM which protected the enzyme against thermal inactivation and increased its suitability for several industrial applications. The stability is rendered due to the formation of high amount of covalent bonds, reduced enzyme mobility and conformational flexibility which in turn inhibits aggregation and unfolding of enzyme protein [20].

The heat inactivation profile of free enzyme, enzyme with free silver nanoparticles and Iamy/Iag-Np/ESM provides a relationship between the enzyme structure and function at a certain temperature (Table 1). Deactivation rate constant (K_d) is an important parameter to promote of an economic bioprocess at commercial scale. Increasing temperature, the $t_{1/2}$ decreases, the D-value decreases and the K_d increases (Table 1). At 60° C, a 22.3-fold increase in $t_{1/2}$ value of α-amylase after immobilization was observed. In addition, at 70° C, D-value of Iamy/Iag-Np/ESM calculated as 2542.05 min. The value was 12.9 fold higher in comparison was found to be higher than that for free enzyme and 2.4 fold higher in comparison to free nanoparticles. The increased $t_{1/2}$ value and D-value confirmed the improved thermal stability after immobilization [22].

The activation energy for denaturation (E_d) is the lowest amount of energy required to initiate the denaturation process of enzyme (Fig. 11 b).

The results indicate that the required energy to denature Iamy/Iag-Np/ESM was 3.75-fold higher than that for free enzyme and 2.8 fold higher than that for enzyme with free nanoparticles.

The thermodynamic parameters as enthalpy (ΔH°), Gibbs free energy (ΔG°), and entropy (ΔS°) were determined for free α-amylase, enzyme with free nanoparticles and Iamy/Iag-Np/ESM. It was observed from the results (Table 1), that with increase in temperature there was a gradual decrease in ΔH° for both forms of enzyme. ΔH° is the total amount of energy required to deactivate the enzyme. At 60° C, ΔH° for the Iamy/Iag-Np/ESM was higher than that of the free enzyme form by 63.83 KJ/mol and of enzyme with silver nanoparticles as 39.18 KJ/mol. Mohapatra *et.al* reported that a positive and higher value of Ed and ΔH° gives an indication of high thermal stability of the enzyme [31]. Gibbs free energy is known as the index of the energy required to cross the activation energy barrier of reaction. ΔG° value for the immobilized enzyme was more than the free enzyme indicating that immobilized enzyme requires more energy than free enzyme for thermal inactivation [8]. Table 1 shows there was an increase in the ΔG° value by 8.4 and 7.2 KJ/mol for Iamy/Iag-Np/ESM over free enzyme at 60° and 70° C, respectively. The Entropy (ΔS°) was the alteration in structural disorder upon protein denaturing and was

directly related to enzyme stability [20]. The obtained ΔS° values were negative, meaning that the randomness or disorder decreased in the transition from the native state to the denatured state of the free and immobilized enzyme [32] Zaboli et al. [8] reported that the negative ΔS° values for the immobilized enzyme indicate lack of enzyme aggregation during thermal inactivation. Decreasing ΔS° after immobilization points to high difference in entropy between the native state and the transition state may be due to the stabilization of enzyme conformation [33].

pH stability:

The pH stability for the free and Iamy/Iag-Np/ESM was studied and is presented in Figure 11 b. Iamy/Iag-Np/ESM was significantly more stable than the free enzyme at all tested pH values especially in the alkaline range. The Iamy/Iag-Np/ESM exhibited great stability and retained 85 % and 76% of its initial activity after 60 min at pH 9 and 10 respectively. Similarly the enzyme with free nanoparticles showed 60% and 55% whereas the free enzyme showed 40 % and 30 %, of its initial activity. Furthermore, the residual activity of Iamy/Iag-Np/ESM at pH 11 was 60 % after 60 min whereas the free enzyme lost 85 % of its activity. These results explained that, the immobilization process enhanced the stability and resistance of α-amylase in both acidic and alkaline pH values. Mission *et al* reported that immobilization of enzymes on nano-carriers resulted in stabilization of active site conformation [21].

Operational stability of Iamy/Iag-Np/ESM:

Immobilization processes are fundamental keys for managing reuse of the enzyme over a long period. The Iamy/Iag-Np/ESM can be easily separated from its products and reused many times for hydrolysis of starch. As shown in Figure 11d the Iamy/Iag-Np/ESM could be reused for 15 consecutive cycles with 83.2 % residual activity. The loss in enzyme activity may be related to repetitive encountering of substrate to the active site of immobilized enzyme that affects the binding strength between carrier and immobilized α-amylase [34]. Furthermore, the reuse of immobilized enzyme in the reaction might cause inactivation and denaturation of the enzyme. The present work shows 80% residual activity for [34] where immobilized α-amylase was reused for 21 cycles [34].

Storage stability:

The main driving force for enzyme immobilization is stabilization. Storage of Iamy/Iag-Np/ESM at 4° C for 21 days retained approximately 80 % of its initial activity .Zaboli et al suggested that the multipoint attachment of the carrier surface to the enzyme may enhance stabilization [8]. In addition Misson et al.[21], reported that the nano-environment surrounding enzyme molecules may prevent enzyme from deactivation.

4. Conclusion

The present study encompasses the kinetic behaviour of α-amylase as free enzyme, enzyme with silver nanoparticles and Iamy/Iag-Np/ESM. The characterization of Iamy/Iag-Np/ESM by FTIR and SEM showed successful immobilization of α-amylase enzyme on silver nanoparticles impregnated egg membrane by covalent bonding. Iamy/Iag-Np/ESM showed high stability over a wide range of pH and temperature. Iamy/Iag-Np/ESM showed increased enzymatic activity as compared to the free enzyme. The present study showed that Iamy/Iag-Np/ESM can be stored for about 21 days and can be reused with its retained activity. Compared to the free enzyme, the Iamy/Iag-Np/ESM exhibited lower Ea, lower K_d, higher $t_{1/2}$ and higher D-values. The calculated thermodynamic parameters $\Delta H°$, $\Delta G°$ and $\Delta S°$ demonstrated that covalent binding between enzyme and the silver nanoparticles impregnated egg membrane increased its thermal stability. Moreover, Iamy/Iag-Np/ESM showed higher stability at different wide range of pH values, viz. 5- 11, compared with free enzyme. The Iamy/Iag-Np/ESM was successfully used in batch mode for 15 cycles for effective degradation of starch with about 100 % residual activity. In addition, Iamy/Iag-Np/ESM retained 80 % after 21 days storage at 4° C. The results demonstrate that immobilized biocatalyst (Iamy/Iag-Np/ESM) has the potential for different applications of industrial processes under extreme conditions of wide range of pH and temperature whereas free enzyme has its maximum activity at a very narrow range of pH and temperature. Also Iamy/Iag-Np/ESM can be reused, easily recovered and increased product formation thus proving as a capable heterogeneous catalyst. References

5. Declaration:

The authors declare the work is not published anywhere else

.

6. Ethics approval and consent to participate:

There is no need as clinical trials are not involved in study

7. Consent for publication:

The authors gave their consent for publication

8. Availability of data and material:

The data is available but not attached with manuscript

9. Competing interests
No competing interests

10. Funding:
No funding for the research work carried out

11. Authors' contributions:
All the authors have equally contributed to the paper

12. Conflict of Interest:
The authors declare that there is no conflict of interests regarding the publication of this article.

13. Acknowledgement:
We sincerely thank Department of Chemical engineering, M.S Ramaiah Institute of Technology and Department of Biotechnology, Sir M Visvesvaraya Institute of Technology for the immense support and encouragement to carry out this work.

14. References

[1] N. Sohrabi, N. Rasouli, M. Torkzadeh, Enhanced stability and catalytic activity of immobilized α-amylase on modified Fe3O4 nanoparticles, *Chem. Engin. J.* **240**,426–433(2014).

[2] D.H. Tambekar, S.D. Tambekar, A.V. Rajgire, A.S, Sawale K.K, Isolation and characterization of amylase from Lysinibacillus xylanilyticus from alkaline environment, *Int. J. Resea. Stud. Biosci.* **4**,1–4 (2016).

[3] G. Pandey, D. Munguambe, M. Tharmavaram, D. Rawtani, Y. Agrawal, Halloysite nanotube -an efficient 'nano-support' for the immobilization of α-amylase, *Appl. Clay Sci.* **136**,184–191(2017).

[4] U.V. Sojitra, S.S. Nadar, V.K. Rathod, Immobilization of pectinase onto chitosan magnetic nanoparticles bymacromolecular cross-linker, *Carbohyd. Polym.***157** ,677–685(2017).

[5] H. Eskandarloo, A. Abbaspourrad, Production of galacto-oligosaccharides from whey permeate using β-galactosidase immobilized on functionalized glass beads, *Food Chem.* **25**(1), 115–124(2018).

[6] C.-H. Kuo, Y.-C. Liu, C.-M.J. Chang, J.-H. Chen, C. Chang, C.-J. Shieh, Optimum conditions for lipase immobilization on chitosan-coated Fe3O4 Nanoparticles, *Carbohyd. Polym.* **87**,2538–2545(2012).

[7] V.U. Bindu, A.A. Shanty, P.V. Mohanan, Parameters affecting the improvement of properties and stabilities of immobilized α-amylase on Chitosan-metal oxide composites, *Int. J. Biochem. Biophys.* **6 ,**44–57(2018).

[8] M. Zaboli, H. Raissi, M. Zaboli, F. Farzad, M. Torkzadeh-Mahani, Stabilization of Dlactate dehydrogenase diagnostic enzyme via immobilization on pristine and carboxyl-functionalized carbon nanotubes, a combined experimental and molecular dynamics simulation study, *Arch. Biochem. Biophys.* **661**,178–186(2019).

[9] M. Sajjad, S. ChouΔH0ry, Effect of starch containing organic substrates on alpha amylase production in Bacillus strains, *Afr. J. Microbiol.Res.* **6** ,7285–7291(2012).

[10] G.L. Miller, Use of dinitrosalicylic acid reagent for determination of reducing sugar, *Analy. Chem.* 31 426–428 (1959).

[11] M.M. Bradford, A rapid and sensitive method for the quantitation of microgram quantities of protein utilizing the principle of protein-dye binding, *Anal. Biochem.* **72**, 248–254 (1976).

[12] G.E.A. Awad, A.A. Abd El Aty, A.N. Shehata, M.E. Hassan, M.M. Elnashar, Covalentimmobilization of microbial naringinase using novel thermally stable biopolymer for hydrolysis of naringin, *Biotech* **3,** 6–14(2016).

[13] G.O. Akalin, M. Pulat, Preparation and characterization of nanoporous sodium carboxymethyl cellulose hydrogel beads, , *J. Nanomat.* Article ID 9676949, 1–12 (2018).

[14] G.E.A. Awad, H.R. Wehaidy, A.A. Abd El Aty, M.E. Hassan, A novel alginate–CMC gel beads for efficient covalent inulinase immobilization, Colloid. *Polym. Sci.* **295**, 495–506(2017).

[15] Y. Yuan, X. Luan, X. Rana, M.E. Hassan, D. Dou, Covalent immobilization of cellulase in application of biotransformation of ginsenoside Rb1, *J. Molec. Cat. B: Enzy*. **133,** S525–S532(2016).

[16] E.A. Karam, M.E. Hassan, M.E. Moharam, A.L. Kansoh, Immobilization of Inulinase Produced by Rhizopus oligosporus NRRL 2549 for continuous fructose production, *J. Mater. Environ. Sci.* **9,** 2315–2321(2018).

[17] Wang X.-Y, X.-P. Jiang, Y. Li, S. Zeng, Y.-W. Zhang, Preparation of Fe3O4 chitosan magnetic particles for covalent immobilization of lipase from Thermomyces lanuginosus, *Int. J. Biologi. Macromol*. **75**, 44–50(2015).

[18] R.N. Singh, A. Bahuguna, P. Chauhan, V.K. Sharma, S. Kaur, S.K. Singh, A. Khan, Production, purification and characterization of thermostable α-amylase from soil isolate Bacillus sp. Strain B-10, *J. BioSci. Biotech*. **5**,37–43(2016).

[19] C.S. Hanes, Studies on plant amylases: the effect of starch concentration upon the velocity of hydrolysis by the amylase of germinated barley, *Biochem. J.* **26**,1406–1421(1932).

[20] D.K. Bedade, A.B. Muley, R.S. Singhal, Magnetic cross-linked enzyme aggregates of acrylamidase from Cupriavidus oxalaticus ICTDB921 for biodegradation of acrylamide from

industrial waste water, *Bioresour. Technol. Rep.* **272** , 137–145(2019) .

[21] Robinson PK. Enzymes: principles and biotechnological applications. *Essays in biochemistry*. **15;**59:1(2015).

[22] Polman EM, Gruter GJ, Parsons JR, Tietema A. Comparison of the aerobic biodegradation of biopolymers and the corresponding bioplastics: A review. *Science of The Total Environment*. **20**;(753),141953(2021).

[21] M. Misson, H. Zhang, B. Jin, Nanobiocatalyst advancements and bioprocessing applications, *J. Roy. Soci. Interf.* **12** ,1–20(2015).

[22] R.S. Singh, K. Chauhan, J.F. Kennedy, Fructose production from inulin using fungal inulinase immobilized on 3-aminopropyl-triethoxysilane S.A. Ahmed et al. / *Biotechnology Reports* **26**, 41–52(2020).

[23] Rosdee NA, Masngut N, Shaarani SM, Jamek S, Sueb MS. Enzymatic hydrolysis of lignocellulosic biomass from pineapple leaves by using endo-1, 4-xylanase: Effect of pH, temperature, enzyme loading and reaction time. *In IOP Conference Series: Materials Science and Engineering* **736**(2), 022095 (2020).

[24] Chattopadhyay K, Mazumdar S. Structural and conformational stability of horseradish peroxidase: effect of temperature and pH. *Biochemistry*. **39**(1), 263-70(2000).

[25] Balcão VM, Vila MM. Structural and functional stabilization of protein entities: state-of-the-art. *Advanced Drug Delivery Reviews*. **1**,(93)25-41(2015).

[26] Shemetov AA, Nabiev I, Sukhanova A. Molecular interaction of proteins and peptides with nanoparticles. *ACS nano*. **26;6**(6):4585-602(2012).

[27] Cleland W. Enzyme kinetics. *Annual review of biochemistry*. **36**(1):77-112(1967).

[28] M.-Y. Zhuang, X.-P. Jiang, X.-M. Ling, M.-Q. Xu, Y.-H. Zhu, Y.-W. Zhang, Immobilization of glycerol dehydrogenase and NADH oxidase for enzymatic synthesis of 1,3-dihydroxyacetone with in

situ cofactor regeneration, *J. Chem. Technol. Biotech.* **93**, 2351–2358(2018).

[29] S.A. Ahmed, F.A. Mostafa, M.A. Ouis, Enhancement stability and catalytic activity of immobilized α-amylase using bioactive phospho-silicate glass as a novel inorganic support, *Int. J. Biol. Macromol.* **112** ,371–382(2018).

[30] S.A. Ahmed, W.A. Abdel Wahab, S.A.M. Abdel-Hameed, Comparative study in kinetics and thermodynamic characteristics of immobilized caseinase on novel support from basalt by physical adsorption and covalent binding, *Biocat. Agricult. Biotech.* **18**, 101028 (2019)

[31] B.R. Mohapatra, Kinetic and thermodynamic properties of alginate lyase and cellulaseco-produced by Exiguobacterium sp. Alg-S5, *Int. J. Biol. Macromol*. **98** ,103–110(2017).

[32] M.M. Ferreira, F.L.B. Santiago, N.A.G. daSilva, J.H.H. Luiz, R. Fernandéz-Lafuente, A.A. Mendes, D.B. Hirata, Different strategies to immobilize lipase from Geotrichum candidum: Kinetic and thermodynamic studies, *Process Biochem.* **67**, 55–63(2018).

[33] H.R. Wehaidy, M.A. Abdel-Naby, W.G. Shousha, M.I.Y. Elmallah, M.M. Shawky, Improving the catalytic, kinetic and thermodynamic properties of Bacillus subtilis KU710517 milk clotting enzyme via conjugation with polyethylene glycol, Int. J. Biol. Macromol. 111 (2018) 296–301.

[34] M. Defaei, A.T. Kafrani, M. Miroliaei, P. Yaghmaei, Improvement of stability and reusability of α-amylase immobilized on naringin functionalized magnetic nanoparticles:Arobustnanobiocatalyst, *Int.J.Biol. Macromol*.**113**,354–360(2018).

[35] Ovais, M., Khalil, A.T., Islam, N.U., Ahmad, I., Ayaz, M., Saravanan, M., Shinwari, Z.K. and Mukherjee, S., Role of plant phytochemicals and microbial enzymes in biosynthesis of metallic nanoparticles. *Applied microbiology and biotechnology*, **102**(16), 6799-6814,(2018).

[36] Maksoud, MIA Abdel, Mohamad Bekhit, Dina M. El-Sherif, Ahmed R. Sofy, and Mahmoud R. Sofy. "Gamma radiation-induced synthesis of a novel chitosan/silver/Mn-Mg ferrite nanocomposite and its impact on cadmium accumulation and translocation in brassica plant growth." *International Journal of Biological Macromolecules* **194**,306-316 (2022).

[37] Abu-Shahba, Mahmoud S., Mahmoud M. Mansour, Heba I. Mohamed, and Mahmoud R. Sofy. "Effect of biosorptive removal of cadmium ions from hydroponic solution containing indigenous garlic peel and mercerized garlic peel on lettuce productivity." *Scientia Horticulturae* **293**,110727 (2022).

[38] Fouda, H.M. and Sofy, M.R.. Effect of biological synthesis of nanoparticles from Penicillium chrysogenum as well as traditional salt and chemical nanoparticles of zinc on canola plant oil productivity and metabolic activity. *Egyptian Journal of Chemistry*, *65*(3),1-2(2022).